(13) Nemoto, N.; Landry, M. R.; Noh, I.; Kitano, T.; Wesson, J. A.; Yu, H. *Macromolecules* **1985**, *18*, 308.
(14) Amis, E. J.; Han, C. C.; Matsushita, Y. *Polymer* **1984**, *25*, 650.
(15) Van Krevelen, D. W. "Properties of Polymers", 2nd ed.; Elsevier: Amsterdam, 1976; p 339.
(16) Smith, B. A.; Samulski, E. T.; Yu, L.-P.; Winnik, M. A., *Macromolecules*, in press.
(17) Smith, B. A.; Samulski, E. T.; Yu, L.-P.; Winnik, M. A. *Phys. Rev. Lett.* **1984**, *52*, 45.
(18) Smith, B. A. *Macromolecules* **1982**, *15*, 469.
(19) Smith, B. A.; McConnell, H. M. *Proc. Natl. Acad. Sci. U.S.A.* **1978**, *75*, 2759.
(20) Smith, L. M.; Smith, B. A.; McConnell, H. M. *Biochemistry* **1979**, *18*, 2256.
(21) Livigni, R. A.; Herold, R. J.; Eliner, O. C.; Aggarwal, S. L. In "Polyethers"; Vandenberg, E. J., Ed.; American Chemical Society, Washington, DC, 1975; Adv. Chem. Ser. No. 6, p 20.
(22) von Meerwall, E.; Grigsby, J.; Tomich, D.; van Antwerp, R. *J. Polym. Sci., Polym. Phys. Ed.* **1982**, *20*, 1037.
(23) Antonietti, M.; Coutandin, J.; Sillescu, H. *Makromol. Chem., Rapid Commun.* **1984**, *5*, 525.
(24) Fixman, M.; Peterson, J. M. *J. Am. Chem. Soc.* **1964**, *86*, 3524.
(25) de Gennes, P.-G. *Phys. Today* **June 1983**, *36*, 33.
(26) Flory, P. G. *J. Chem. Phys.* **1949**, *17*, 303.
(27) Evans, K. E.; Edwards, S. F. *J. Chem. Soc., Faraday Trans. 2* **1981**, *77*, 1913.
(28) Rubinstein, M.; Helfand, E. *J. Chem. Phys.* **1985**, *82*, 2477.
(29) Graessley, W. W.; Edwards, S. F. *Polymer* **1981**, *22*, 1329.

A Long, Regular Polypeptide 3_{10}-Helix†

C. Toniolo* and G. M. Bonora

Biopolymer Research Center, C.N.R., Department of Organic Chemistry, University of Padova, 35131 Padova, Italy

A. Bavoso, E. Benedetti,* B. Di Blasio, V. Pavone, and C. Pedone

Department of Chemistry, University of Naples, 80134 Naples, Italy.
Received August 1, 1985

ABSTRACT: The infrared absorption and ^1H nuclear magnetic resonance analyses of chloroform solutions of the terminally blocked homooctapeptide from the $C_{\alpha,\alpha}$-dimethylated α-aminoisobutyric acid residue are consistent with the presence of a 3_{10}-helical structure of high thermal stability. The crystal structure of the octapeptide, obtained by X-ray diffraction, indicates the formation of a 3_{10}-helix, stabilized by six consecutive intramolecular N—H···O=C H bonds of the C_{10}-III (or III′) type. This represents the first observation at atomic resolution of a *regular* 3_{10}-helix larger than two complete turns. Packing of the octapeptide molecules gives rise to a channel in which the solvent (methanol and water) molecules are accommodated.

1. Introduction

The polypeptide 3_{10}-helix, first proposed by Donohue in the early 1950s[15] has a three-residue repeat and a H bond between the C=O group of residue i and the N–H group of residue $i + 3$ [type III (or III′) C_{10}-form or β-bend].[53,55,62] Its ϕ,φ torsion angles are approximately ±60°, ±30°, within the same energy minimum in the conformational map as the α-(3.6_{13}) helix.[13,47,63] However, the H-bonding schemes are significantly different in the two types of helices, being of the $i \leftarrow i + 4$ (C_{13}-form or α-bend[55]) in the α-helix. For a long periodic structure formed by C^{α}-*mono*alkylated α-amino acid residues with the same chirality at the α-carbon atom, the 3_{10}-helix is energetically considerably less favorable than the α-helix.[13,47,63] Therefore, it is not surprising that only short pieces of approximately 3_{10}-helix (particularly at the C terminus of an α-helix) have been found in protein crystal structure analyses[11,13,34,47,49] (for recent examples, see ref 14, 27, and 65).

More recently, by theoretical[1,4,10,33,38,40,42,60,61] as well as experimental[3,8,9,22,23,26,36,44,50,52,56,58,61] studies it has been shown that the ϕ,φ angles of the achiral Aib (α-aminoisobutyric acid) residue, the prototype of the $C^{\alpha,\alpha}$-*di*alkylated α-amino acids, are restricted to values near those associated with either right- or left-handed α- or 3_{10}-helices, unless it is part of a strained cyclic compound.[21] The X-ray diffraction structures of Aib homopeptides to the pentamer have provided examples of short (less than two complete turns) 3_{10}-helical conformations in the solid state.[3,44,52,56,61] Our recent solution conformational analysis of monodispersed, terminally blocked $(Aib)_n$ homooligopeptides to the dodecamer is strongly in favor of the formation of fully developed, stable 3_{10}-helices in chloroform, starting from the octamer.[58]

In this paper we present the results of a conformational investigation in $CDCl_3$ solution of the terminally blocked Aib homooctapeptide, *p*-BrBz-$(Aib)_8$-O-*t*-Bu (*p*-BrBz = *p*-bromobenzoyl, O-*t*-Bu = *tert*-butoxy) by using infrared (IR) absorption and ^1H nuclear magnetic resonance (NMR). We extended the study of the structural preferences of this octapeptide to the crystal state by means of X-ray diffraction. This investigation represents the first observation at atomic resolution of a long (more than two complete turns), *regular* 3_{10}-helix and allowed us to characterize this important peptide ordered secondary structure in detail.

2. Materials and Methods

(a) Peptide Synthesis. *p*-BrBz-Aib-OH. This compound was synthesized from *p*-BrBz-Cl and H-Aib-OH in an aqueous NaOH–acetone mixture: yield 95%; mp 226–227 °C (from ethyl acetate–petroleum ether); thin-layer chromatography (silica gel plates 60F-254, Merck Darmstadt) R_{f1} (9:1 $CHCl_3$–ethanol) 0.10, R_{f2} (3:1:1 1-butanol–acetic acid–water) 0.80. Anal. Calcd for $C_{11}H_{12}NO_3Br$: C, 46.2; H, 4.2; N, 4.9; Br, 27.9. Found: C, 46.2; H, 4.2; N, 4.9; Br, 28.0. The crystal structure has recently been solved by X-ray diffraction.[59]

Oxazolone from *p*-BrBz-Aib-OH. This compound was synthesized from *p*-BrBz-Aib-OH in acetic anhydride at 120 °C for 20 min:[58] yield 96%; mp 106–107 °C (from hot benzene); R_{f1} 0.95. Anal. Calcd for $C_{11}H_{10}NO_2Br$: C, 49.3; H, 3.8; N, 5.2; Br, 29.8. Found: C, 48.8; H, 3.9; N, 5.1; Br, 29.2. The crystal structure of this compound has recently been solved by X-ray diffraction.[59]

† This is part 143 in the series "Linear Oligopeptides". For part 142, see ref 57.

0024-9297/86/2219-0472$01.50/0

p-BrBz-Aib-O-t-Bu. This compound was synthesized from p-BrBz-Aib-OH and isobutene in anhydrous methylene chloride in the presence of a catalytic amount of H_2SO_4:[58] yield 61%; mp 144–145 °C (from ethyl acetate–petroleum ether); R_{f1} 0.90, R_{f2} 0.90. Anal. Calcd for $C_{15}H_{20}NO_3Br$: C, 52.6; H, 5.9; N, 4.1; Br, 23.3. Found: C, 52.1; H, 5.8; N, 4.0; Br, 23.1.

p-BrBz-(Aib)$_2$-O-t-Bu. This compound was prepared from the oxazolone from p-BrBz-Aib-OH and H-Aib-O-t-Bu[58] in anhydrous acetonitrile under reflux for 8 h:[58] yield 65%; mp 131–132 °C (from ethyl ether–petroleum ether); R_{f1} 0.90, R_{f2} 0.90. Anal. Calcd for $C_{19}H_{27}N_2O_4Br$: C, 53.4; H, 6.4; N, 6.6; Br, 18.7. Found: C, 53.5; H, 6.4; N, 6.6; Br, 18.9.

p-BrBz-(Aib)$_2$-OH. This compound was prepared from p-BrBz-(Aib)$_2$-O-t-Bu in the presence of trifluoroacetic acid for 1 h:[58] yield 97%; mp 234–235 °C (from ethyl acetate–petroleum ether); R_{f1} 0.10, R_{f2} 0.80. Anal. Calcd for $C_{15}H_{19}N_2O_4Br$: C, 48.5; H, 5.2; N, 7.6; Br, 21.5. Found: C, 47.9; H, 5.1; N, 7.5; Br, 21.3.

Oxazolone from p-BrBz-(Aib)$_2$-OH. This compound was prepared from p-BrBz-(Aib)$_2$-OH in acetic anhydride at 120 °C for 20 min:[58] yield 91%; mp 125–126 °C (from hot benzene); R_{f1} 0.95. Anal. Calcd for $C_{15}H_{17}N_2O_3Br$: C, 51.0; H, 4.9; N, 7.9; Br, 22.6. Found: C, 50.2; H, 4.8; N, 7.8; Br, 22.1.

p-BrBz-(Aib)$_3$-O-t-Bu. This compound was synthesized from the oxazolone from p-BrBz-(Aib)$_2$-OH and H-Aib-O-t-Bu[58] in anhydrous acetonitrile under reflux for 8 h:[58] yield 65%; mp 191–192 °C (from ethyl ether–petroleum ether); R_{f1} 0.55, R_{f2} 0.90. Anal. Calcd for $C_{23}H_{34}N_3O_5Br$: C, 53.9; H, 6.7; N, 8.2; Br, 15.6. Found: C, 53.3; H, 6.7; N, 8.1; Br, 15.4.

p-BrBz-(Aib)$_3$-OH. This compound was prepared from p-BrBz-(Aib)$_3$-O-t-Bu in the presence of trifluoroacetic acid for 1 h:[58] yield 94%; mp 190–192 °C (from ethyl acetate–petroleum ether); R_{f1} 0.00; R_{f2} 0.70. Anal. Calcd for $C_{19}H_{26}N_3O_5Br$: C, 50.0; H, 5.7; N, 9.2; Br, 17.5. Found: C, 50.1; H, 5.8; N, 9.1; Br, 17.3.

Oxazolone from p-BrBz-(Aib)$_3$-OH. This compound was prepared from p-BrBz-(Aib)$_3$-OH in acetic anhydride at 120 °C for 10 min:[58] yield 62%; mp 185–186 °C (from hot benzene); R_{f1} 0.55. Anal. Calcd for $C_{19}H_{24}N_3O_4Br$: C, 52.1; H, 5.5; N, 9.6; Br, 18.2. Found: C, 51.6; H, 5.4; N, 9.5; Br, 18.0.

p-BrBz-(Aib)$_8$-O-t-Bu. This compound was synthesized from the oxazolone from p-BrBz-(Aib)$_3$-OH and H-(Aib)$_5$-O-t-Bu[58] in anhydrous acetonitrile under reflux for 12 h:[58] yield 37%; mp 323–324 °C; R_{f1} 0.35, R_{f2} 0.85. Anal. Calcd for $C_{43}H_{69}N_8O_{10}Br$: C, 55.1; H, 7.4; N, 11.9; Br, 8.5. Found: C, 54.6; H, 7.3; N, 11.8; Br, 8.4.

(b) Infrared Absorption. Infrared absorption spectra were recorded with a Perkin-Elmer Model 580B spectrophotometer equipped with a Perkin-Elmer Model 3600 IR data station. The band positions are accurate to ±1 cm^{-1}. Cells with path lengths 0.1 and 1.0 cm (with CaF_2 windows) were used. Spectrograde deuteriochloroform (99.8% d) was purchased from Merck. For the measurements at variable temperature a Specac Model P/N 21.000 (Analytical Accessories, Ltd., Orpington, Kent, U.K.) thermostatically controlled cell was employed. Spectra were taken for a 1.0-mm path length sample cell with AgCl windows. Temperature was measured directly in the sample by means of a thermocouple. Because some of the bands exhibited sensitivity to humidity, the presence of which was revealed by the occurrence of significant absorptions at 3670 and 3580 cm^{-1}, great care was paid to ensure the absence of water in the solvent.

(c) ^{1}H Nuclear Magnetic Resonance. The ^{1}H nuclear magnetic resonance spectra were recorded with a Bruker Model WP200SY spectrometer. Measurements were carried out in deuteriochloroform (99.96% d; Merck) and dimethyl sulfoxide (99.96% d_6; Stohler) with tetramethylsilane as the internal standard. The free radical TEMPO (2,2,6,6-tetramethyl-1-piperidinyloxy) was purchased from Sigma.

(d) X-ray Diffraction. Crystals of p-BrBz-(Aib)$_8$-O-t-Bu were grown from a mixture of methylene chloride and methanol by slow evaporation at room temperature. Preliminary oscillation and Weissenberg photographs were taken to establish the crystal symmetry and space group. Determination of the cell constants and collection of the X-ray intensity data were performed on a CAD4 Enraf-Nonius diffractometer at the Centro di Metodologie Chimico-Fisiche of the University of Naples, equipped with PDP8/E and PDP11/34 digital computers. For the structure determination and refinement, the structure determination programs (SDP) package was used. Unit cell parameters were obtained with the orientation matrix for data collection by means of a least-squares procedure of the angular parameters of 25 centered high-angle reflections. A summary of the crystal data is given in Table I.

Table I
Crystallographic Data for p-BrBz-(Aib)$_8$-O-t-Bu

mol formula	$C_{43}H_{69}N_8O_{10}\cdot H_2O\cdot 3CH_3OH$
mol weight (amu)	1052.13
crystal system	triclinic
space group	$P\bar{1}$
Z, molecules/unit cell	2
a, Å	11.001 (4)
b, Å	16.265 (4)
c, Å	16.681 (4)
α, deg	101.36 (2)
β, deg	90.82 (3)
γ, deg	95.10 (3)
V, Å^3	2984.3
d(calcd), g/cm^3	1.199
d(exptl), g/cm^3 (by flotation)	1.20
radiation	Cu Kα, λ = 1.5418 Å
no. of independent reflections	11043
reflections with $I > 3.0\sigma(I)$	3799
final R value	0.097
temp, °C	23, ambient

The analysis of the peak profiles suggested an ω–2θ scan mode with a scan angle $\Delta\omega = (1.0 + 0.15 \tan\theta)°$; background counts were taken in an additional area of $\Delta\omega/4°$ on both sides of the main scan with the same scan speed for each reflection. A crystal-to-counter distance of 368 mm was used with horizontal and vertical counter entrance aperture of 4 mm and $(3.5 + 0.5 \tan\theta)°$, respectively. The tube placed between the goniometer head and the detector was evacuated with a vacuum pump. Prescan runs were made at a speed of 3.5°/min.

Reflections with a net intensity $I \leq 0.5\sigma(I)$ were flagged as "weak"; those having $I > 0.5\sigma(I)$ were measured at lower speed (1.0–3.5°/min) depending on the value of $\sigma(I)/I$. Two intensity control reflections were measured every 60 min of X-ray exposure time in order to monitor the crystal and the electronic stability; no significant change in intensity was observed during data collection.

Orientation matrix checks were made with respect to the scattering vectors of four well-centered reflections every 200 reflections; reorientation was made by using 25 high-angle reflections if the displacements of the measured scattering vector exceeded the calculated value of 0.15°. In the range 1–70° of θ explored, 11 043 reflections were collected; of those, 3799 with a net intensity greater than $3.0\sigma(I)$ were considered as observed and used in the subsequent calculations. All reflections were corrected for Lorentz and polarization effects.

The structure was solved by means of direct methods, using MULTAN.[24] The E map of the set of phases with the best combined figures of merit revealed the position of most of non-hydrogen atoms. The remaining atoms were located by subsequent Fourier synthesis. The structure was refined by a full-matrix least-squares procedure, minimizing the quantity $\sum w(F_o^2 - F_c^2)^2$ with weights w equal to $1/\sigma(F_o^2)$. All heavy atoms were refined with anisotropic temperature factors. Hydrogen atoms were introduced in their stereochemically expected positions with isotropic temperature factors equal to the equivalent B factor of the atom to which each of them is linked.

Refinement was ended when the shifts in the atomic coordinates and anisotropic temperature factors for the heavy atoms were less than $^1/_5$ and $^1/_3$ of the corresponding standard deviations, respectively. The atomic scattering factors, with the real and imaginary dispersion corrections, for all atomic species were calculated according to Cromer and Waber.[12] A final R of 0.097 for the 3799 observed reflections was obtained. The final atomic parameters of the non-hydrogen atoms are listed in Table II.

3. Results

(a) Solution Study. The solution-preferred conformation of the terminally blocked homooctapeptide p-BrBz-(Aib)$_8$-O-t-Bu was examined in a solvent of low po-

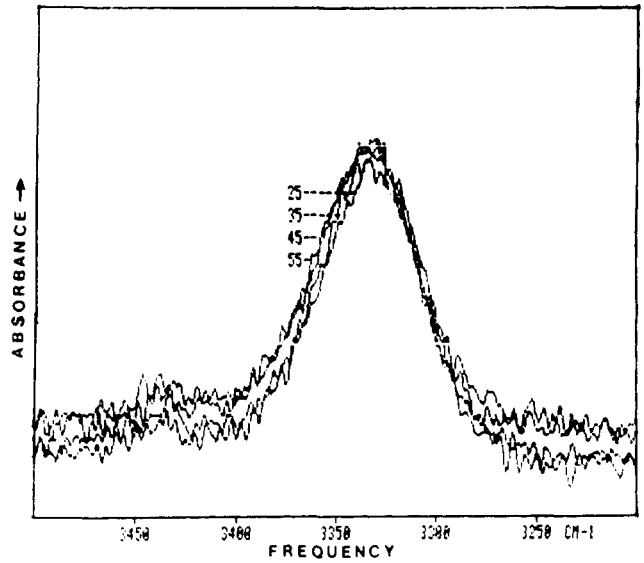

Figure 1. Temperature dependence of the IR absorption spectrum of *p*-BrBz-(Aib)$_8$-O-*t*-Bu in the 3500–3200-cm^{-1} region. Concentration 0.6 × 10^{-3} M in $CDCl_3$ solution.

larity ($CDCl_3$) by using IR absorption and ^{1}H NMR (Figures 1–3). At 0.6 × 10^{-3} M concentration the IR absorption spectrum in the N–H stretching region (Figure 1) shows a weak band at 3435 cm^{-1}, assigned to free (solvated) amide and peptide N–H groups.[3,6,7,35,39,43,57,58,64] The strong absorption associated with H-bonded N–H groups is seen at 3327 cm^{-1}.[3,6,7,35,39,43,57,58,64] To investigate the concentration effect, spectra were also recorded at 0.75 × 10^{-3} and 0.15 × 10^{-3} M concentrations (not shown). A comparison of the A_H/A_F values, where A_H/A_F is the ratio of integrated intensity of the band of H-bonded N–H groups to free N–H groups,[3,6,7,35,57,58,64] indicates that the octapeptide tends to self-aggregate above 0.6 × 10^{-3} M concentration. The high A_H/A_F value, even in the absence of self-aggregation, points to the occurrence of highly folded, intramolecularly H-bonded species. The C=O stretching bands are seen at 1724 cm^{-1} (*tert*-butyl ester[3,6,58]) and 1662 cm^{-1} (amide and peptide groups[6,57,58]) (not shown). The marked thermal stability of the unaggregated, folded species (concentration 0.6 × 10^{-3} M) is illustrated in Figure 1. This IR absorption analysis has shown that intermolecular as well as intramolecular H bonds occur in $CDCl_3$ solution. In addition, free N–H groups are also present.

The ^{1}H NMR study of the octapeptide was performed in $CDCl_3$ solution as a function of concentration,[6,57,58] temperature,[6,45,54] addition of the strong H-bonding acceptor solvent[32] dimethyl sulfoxide (Me_2SO)[41] and the free radical 2,2,6,6-tetramethyl-1-piperidinyloxy (TEMPO)[29] (Figures 2 and 3).

In the N–H region of the spectrum of this *homo*peptide there are no resonances that are unambiguously assigned.[6,7,39,58] However, by analogy with the chemical shifts of the corresponding protons of the lowest members of the *p*-BrBz-(Aib)$_n$-O-*t*-Bu series (not shown) and of a variety of model compounds,[6,7,57,58] we tentatively assign the only two resonances below 7.00 ppm to the N(1)H and N(2)H protons. It is pertinent to mention here that we number the amino acid residues as usual, i.e., from the N terminus of the peptide chain, so that the proton attached to the nitrogen of the N-terminal residue is labeled N(1)H.[6,7,45,54,57,58]

An analysis of the spectrum as a function of concentration (Figure 2) shows that a dilution from 0.75 × 10^{-3} to 0.6 × 10^{-3} M produces a significant variation (to higher

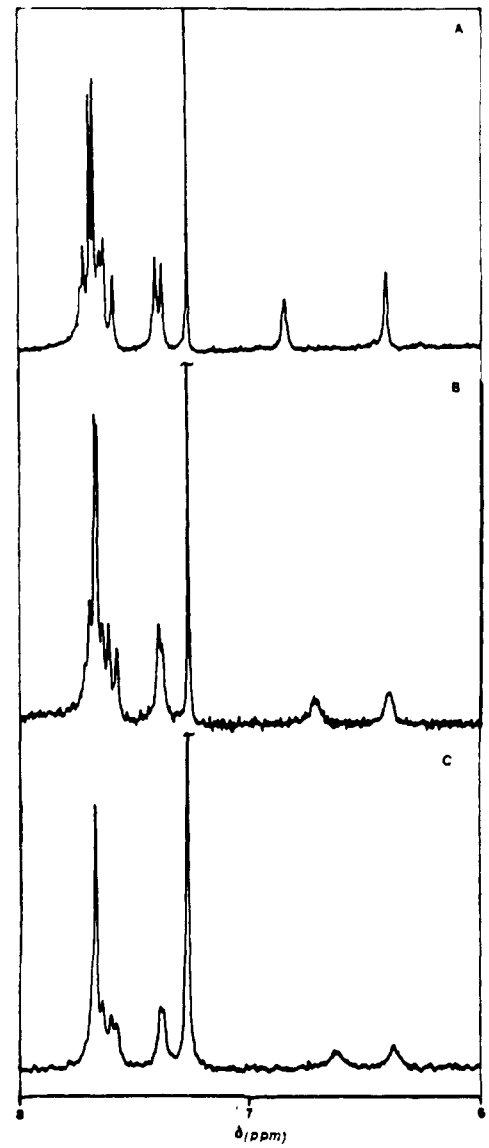

Figure 2. Partial 200-MHz NMR spectra (low-field region) of *p*-BrBz-(Aib)$_8$-O-*t*-Bu in $CDCl_3$ solution as a function of concentration: (a) 0.75 × 10^{-3}, (b) 0.6 × 10^{-3}, and (c) 0.15 × 10^{-3} M. Temperature 293 K.

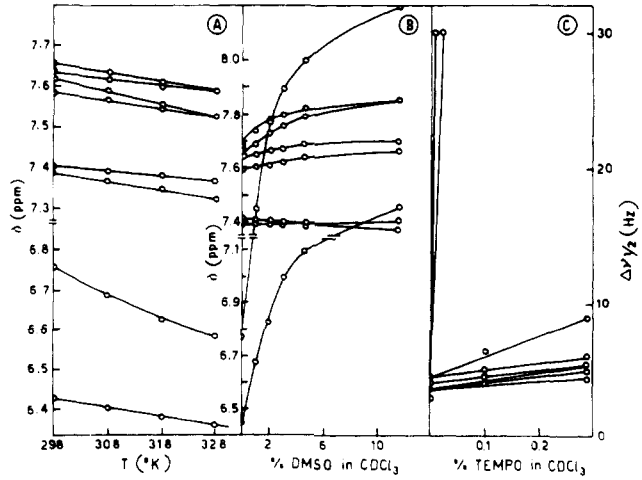

Figure 3. (A) Plot of NH chemical shifts in the ^{1}H NMR spectra of *p*-BrBz-(Aib)$_8$-O-*t*-Bu vs. temperature in $CDCl_3$. (B) Plot of NH chemical shifts of the same peptide vs. increasing percentages of Me_2SO to the $CDCl_3$ solution (volume/volume). (C) Plot of bandwidth of the NH signal of the same peptide vs. increasing percentages of TEMPO (weight/volume) in $CDCl_3$. Concentration 0.6 × 10^{-3} M.

Table II
Final Atomic Parameters and Their Standard Deviations (in Parentheses) for *p*-BrBz-$(Aib)_8$-O-*t*-Bu

atom	x/a (×10⁴)	y/b (×10⁴)	z/c (×10⁴)	B_{eq}	atom	x/a (×10⁴)	y/b (×10⁴)	z/c (×10⁴)	B_{eq}
Br	1691 (2)	1136 (2)	10968 (1)	9.52 (7)	$C_5^{\beta,L}$	147 (16)	3958 (14)	2609 (12)	8.4 (6)
C(1)	2002 (11)	1225 (7)	9383 (6)	3.5 (3)	$C_5^{\beta,D}$	−506 (15)	4410 (10)	4039 (9)	6.7 (4)
C(2)	3122 (14)	1540 (11)	9708 (8)	5.3 (4)	C_5'	−1870 (11)	3421 (8)	3016 (7)	3.9 (3)
C(3)	3348 (13)	1586 (13)	8882 (7)	6.8 (5)	O_5	−2335 (9)	3763 (6)	2508 (5)	5.3 (2)
C(4)	2549 (13)	1238 (10)	8286 (7)	3.9 (3)	N_6	−2509 (10)	2850 (8)	3349 (5)	4.7 (3)
C(5)	1381 (14)	935 (9)	8499 (8)	5.3 (4)	C_6^{α}	−3787 (14)	2612 (13)	3104 (8)	7.0 (5)
C(6)	1194 (14)	878 (12)	9289 (8)	6.3 (5)	$C_6^{\beta,L}$	−4570 (16)	3277 (16)	3460 (9)	7.4 (4)
C(7)	2644 (13)	1275 (13)	7406 (8)	6.1 (4)	$C_6^{\beta,D}$	−4088 (14)	1815 (13)	3500 (8)	7.6 (5)
O(1)	1784 (8)	1204 (7)	6942 (5)	5.4 (3)	C_6'	−3956 (10)	2274 (8)	2200 (9)	4.5 (3)
N_1	3798 (10)	1393 (8)	7115 (5)	5.2 (3)	O_6	−4961 (8)	2332 (8)	1869 (6)	6.9 (3)
C_1^{α}	4059 (11)	1343 (9)	6243 (7)	4.7 (4)	N_7	−3056 (9)	1947 (8)	1783 (7)	4.3 (2)
$C_1^{\beta,L}$	3680 (14)	410 (11)	5745 (9)	5.5 (4)	C_7^{α}	−3127 (11)	1594 (8)	920 (7)	4.3 (4)
$C_1^{\beta,D}$	5442 (11)	1549 (9)	6186 (7)	4.9 (4)	$C_7^{\beta,L}$	−4005 (17)	831 (14)	690 (8)	8.3 (6)
C_1'	3349 (10)	1958 (9)	5914 (8)	4.4 (4)	$C_7^{\beta,D}$	−1823 (14)	1408 (11)	661 (9)	5.7 (4)
O_1	2998 (7)	1801 (6)	5181 (4)	5.3 (2)	C_7'	−3397 (12)	2281 (9)	404 (7)	3.8 (3)
N_2	3254 (9)	2707 (8)	6429 (6)	4.0 (3)	O_7	−3695 (9)	2058 (7)	−333 (5)	6.0 (3)
C_2^{α}	2659 (13)	3390 (10)	6192 (8)	4.9 (3)	N_8	−3166 (10)	3080 (8)	765 (6)	5.1 (3)
$C_2^{\beta,L}$	3436 (13)	3838 (11)	5615 (11)	6.9 (5)	C_8^{α}	−3370 (13)	3756 (12)	317 (8)	6.0 (4)
$C_2^{\beta,D}$	2472 (14)	4024 (10)	7022 (9)	6.0 (4)	$C_8^{\beta,L}$	−2851 (18)	4560 (13)	857 (10)	6.5 (4)
C_2'	1380 (11)	3087 (8)	5780 (7)	3.4 (3)	$C_8^{\beta,D}$	−4697 (12)	3757 (10)	98 (8)	6.8 (5)
O_2	918 (7)	3490 (6)	5329 (4)	5.4 (2)	C_8'	−2632 (12)	3635 (10)	−465 (7)	5.5 (4)
N_3	768 (9)	2446 (8)	6024 (6)	4.5 (3)	O_8	−2949 (11)	3694 (9)	−1129 (6)	8.8 (4)
C_3^{α}	−457 (16)	2019 (14)	5683 (10)	6.9 (5)	O(2)	−1476 (8)	3476 (7)	−313 (5)	6.2 (3)
$C_3^{\beta,L}$	−1401 (13)	2709 (12)	5963 (9)	6.9 (4)	C(8)	−547 (18)	3340 (14)	−951 (10)	7.5 (5)
$C_3^{\beta,D}$	−742 (14)	1274 (13)	5973 (9)	8.7 (6)	C(9)	615 (17)	3262 (16)	−482 (14)	11.9 (7)
C_3'	−482 (13)	1833 (10)	4766 (7)	4.9 (4)	C(10)	−415 (17)	4069 (16)	−1360 (12)	9.8 (7)
O_3	−1454 (8)	1777 (8)	4369 (5)	6.4 (3)	C(11)	−923 (23)	2476 (17)	−1544 (12)	9.2 (6)
N_4	578 (10)	1730 (9)	4388 (6)	5.6 (3)	O_w	4931 (12)	6521 (10)	2253 (9)	13.1 (5)
C_4^{α}	683 (14)	1546 (12)	3503 (8)	7.2 (4)	O_{M1}	3999 (9)	8881 (7)	1926 (6)	7.8 (3)
$C_4^{\beta,L}$	235 (17)	734 (10)	3094 (8)	7.6 (6)	C_{M1}	3313 (19)	9517 (13)	2010 (12)	10.5 (7)
$C_4^{\beta,D}$	2064 (14)	1766 (14)	3315 (7)	7.4 (6)	O_{M2}	3513 (17)	3630 (13)	1968 (11)	14.7 (7)
C_4'	51 (16)	2223 (11)	3126 (8)	3.8 (3)	C_{M2}	2668 (33)	3494 (32)	1292 (22)	18.0 (10)
O_4	−450 (8)	2007 (6)	2425 (5)	4.4 (2)	O_{M3}	3987 (19)	5208 (15)	2936 (16)	19.1 (9)
N_5	33 (10)	3006 (8)	3573 (5)	4.5 (3)	C_{M3}	3294 (38)	5209 (34)	3690 (39)	27.2 (18)
C_5^{α}	−536 (11)	3662 (8)	3310 (7)	4.4 (4)					

fields) of the chemical shifts of the N(1)H and N(2)H protons, less evident for the proton at higher fields. For the six protons at lower fields the concentration effect is negligible. We conclude that at a concentration higher than 0.6×10^{-3} M the octapeptide self-aggregates and that in this process the N(1)H and N(2)H groups are those acting as H-bonding donors.[6,57,58]

The solvent accessibilities of the NH protons, indicative of a possible participation to intramolecular H bonds, were examined as a function of temperature[6,45,54] and addition of Me_2SO[41] and TEMPO[29] to the $CDCl_3$ solution (concentration 0.6×10^{-3} M) (Figure 3). Two classes of NH protons are observed: (i) the N(1)H and N(2)H protons, whose chemical shifts are sensitive to heating and, particularly, to the addition of Me_2SO and whose resonances broaden significantly upon addition of TEMPO; and (ii) all other NH protons, whose resonances, in terms of chemical shifts and line width, are only marginally sensitive to environmental changes.

On the basis of these ^1H NMR results, it is evident that at relatively high concentration ($>0.6 \times 10^{-3}$ M) in $CDCl_3$ solution the N(1)H as well as the N(2)H protons of the octapeptide are involved in the intermolecular H-bonding scheme, i.e., in the self-aggregation process, whereas all other protons form intramolecular H bonds. The intramolecular H-bonding scheme does not change upon self-aggregation and is stable to either heating or addition of Me_2SO and TEMPO. Since all NH protons, beginning from the N(3)H proton, form intramolecular H bonds, it may be concluded that the ordered secondary structure adopted by the Aib homooctapeptide in $CDCl_3$ solution is the 3_{10}-helix.[6,7,39,57,58] However, we wish to stress the point that, in the absence of unambiguous assignments for NH protons and detailed information on the ϕ torsion angles from $J_{NH-\alpha-CH}$ coupling constants (the compound under examination is a *homo*peptide and the constituent amino acid does not possess the α-CH proton), these conclusions are only tentative, although corroborated by the results of the X-ray diffraction analysis (see below) and the known conformational rigidity of Aib-rich polypeptides.

(b) Solid-State Study. The molecular structure of *p*-BrBz-$(Aib)_8$-O-*t*-Bu is shown in Figure 4. Each molecule, having no chiral atoms, crystallizes with retention of the center of symmetry; thus in each unit cell molecules of both handedness simultaneously occur. We incorporated the *p*-BrBz group at the N terminus to help solve the phase problem in the X-ray diffraction analysis, since it incorporates a suitable heavy atom (Br).

Bond lengths (Table III) and bond angles (Table IV) are in good agreement with literature values for *p*-bromobenzoyl,[37,48] peptide[2,28] and ester group,[16,51] and the Aib residue.[38,61] In particular, the inspection of the bond angles involving the C^{α} atoms confirmed the expected asymmetry.[38,61] The succession of similar pairs of ϕ,φ values[25] (mean values = ±54.0° and ±28.4°, respectively) (Table V) along the chain gives rise to a helical structure, which can be described as a 3_{10}-helix, very close to the ideal case $(\phi,\varphi) = (\pm 60°, \pm 30°)$.[13,15,47] There are six successive intramolecular N—H···O=C H bonds of the C_{10}-III (or C_{10}-III′) type.[53,55,62] The range of observed N···O distances is 2.94–3.04 Å (mean value = 2.99 Å)[46] (Table VI). The deviations of the ω angles from the ideal value of the trans planar unit (180°)[2,28] are extremely small (the average $|\Delta\omega|$ value is 1.7°) (Table VI). In this helix one peptide group is carried into the next to which it is directly chemically linked by a rotation of 120° and an axial translation of 1.95 Å. The pitch is 5.85 Å, and there are three residues per

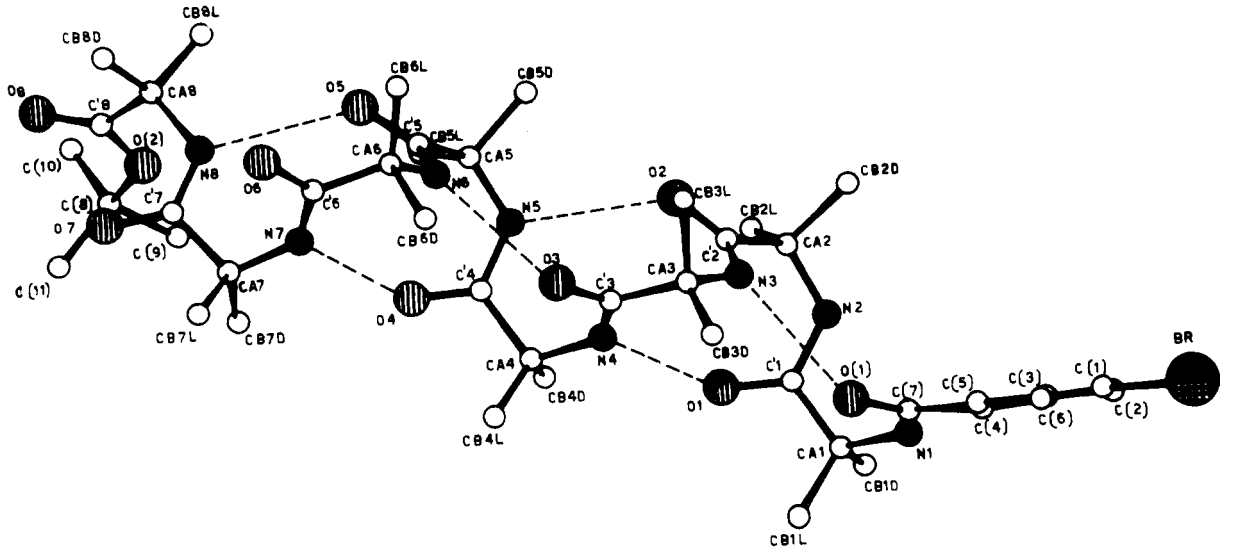

Figure 4. Molecular structure of *p*-BrBz-(Aib)$_8$-O-*t*-Bu. In this figure the left-handed helical molecule is shown. The six intramolecular H bonds of the C_{10} type are indicated as dashed lines.

Table III

Bond Lengths (Å) with ESD's for the Aib Residues in *p*-BrBz-(Aib)$_8$-O-*t*-Bu

	residue							
length	1	2	3	4	5	6	7	8
N_i–C_i^{α}	1.48 (1)	1.45 (2)	1.51 (2)	1.46 (1)	1.42 (2)	1.46 (2)	1.44 (1)	1.48 (2)
C_i^{α}–$C_i^{\beta,L}$	1.60 (2)	1.54 (2)	1.60 (3)	1.40 (2)	1.53 (2)	1.48 (3)	1.49 (2)	1.50 (2)
C_i^{α}–$C_i^{\beta,D}$	1.54 (2)	1.58 (2)	1.40 (3)	1.58 (2)	1.54 (2)	1.58 (2)	1.54 (2)	1.50 (2)
C_i^{α}–C_i'	1.50 (2)	1.55 (2)	1.50 (2)	1.58 (2)	1.53 (2)	1.50 (2)	1.58 (2)	1.54 (2)
C_i'–O_i	1.25 (1)	1.22 (1)	1.24 (2)	1.26 (1)	1.23 (1)	1.25 (1)	1.24 (1)	1.18 (1)
C_i'–N_{i+1}	1.36 (2)	1.32 (2)	1.34 (2)	1.35 (2)	1.33 (2)	1.31 (2)	1.32 (2)	

Bond Lengths (Å) with ESD's for the N- and C-Terminal Blocking Groups of *p*-BrBz-(Aib)$_8$-O-*t*-Bu and the Solvent Molecules

C(1)–C(2)	1.33 (2)	C_8'–O(2)	1.35 (2)
C(1)–C(6)	1.28 (2)	O(2)–C(8)	1.48 (2)
C(2)–C(3)	1.42 (1)	C(8)–C(9)	1.52 (3)
C(3)–C(4)	1.32 (2)	C(8)–C(10)	1.48 (3)
C(4)–C(5)	1.41 (2)	C(8)–C(11)	1.57 (3)
C(4)–C(7)	1.48 (1)	O_{M1}–C_{M1}[a]	1.32 (2)
C(5)–C(6)	1.36 (1)	O_{M2}–C_{M2}[a]	1.42 (3)
C(7)–O(1)	1.20 (1)	O_{M3}–C_{M3}[a]	1.48 (6)
C(7)–N_1	1.38 (2)		

[a] M1, M2, and M3 indicate the three cocrystallized methanol molecules.

Table IV

Bond Angles (Deg) with ESD's for the Aib Residues in *p*-BrBz-(Aib)$_8$-O-*t*-Bu

	residue							
angle	1	2	3	4	5	6	7	8
C_{i-1}'–N_i–C_i^{α}	124 (2)	123 (2)	126 (2)	124 (2)	124 (2)	120 (2)	125 (2)	121 (2)
N_i–C_i^{α}–C_i'	109 (2)	112 (2)	111 (2)	109 (2)	114 (2)	112 (2)	111 (2)	109 (2)
N_i–C_i^{α}–$C_i^{\beta,L}$	110 (2)	112 (2)	105 (2)	116 (2)	111 (2)	112 (2)	114 (2)	106 (2)
N_i–C_i^{α}–$C_i^{\beta,D}$	107 (2)	105 (2)	111 (2)	107 (2)	108 (2)	102 (2)	107 (2)	111 (2)
C_i'–C_i^{α}–$C_i^{\beta,L}$	110 (2)	109 (2)	107 (2)	110 (2)	107 (2)	116 (2)	111 (2)	107 (2)
C_i'–C_i^{α}–$C_i^{\beta,D}$	112 (2)	108 (2)	110 (2)	101 (2)	108 (2)	104 (2)	101 (2)	110 (2)
$C_i^{\beta,D}$–C_i^{α}–$C_i^{\beta,L}$	109 (2)	110 (2)	113 (2)	112 (2)	108 (2)	109 (2)	111 (2)	113 (2)
C_i^{α}–C_i'–O_i	120 (2)	120 (2)	121 (2)	119 (2)	121 (2)	118 (2)	120 (2)	128 (2)
C_i^{α}–C_i'–N_{i+1}	116 (2)	117 (2)	118 (2)	119 (2)	117 (2)	120 (2)	117 (2)	
O_i–C_i'–N_{i+1}	124 (2)	122 (2)	121 (2)	122 (2)	122 (2)	122 (2)	123 (2)	

Bond Angles (Deg) with ESD's for the N- and C-Terminal Blocking Groups of *p*-BrBz-(Aib)$_8$-O-*t*-Bu

Br–C(1)–C(2)	115 (2)	Br–C(1)–C(6)	118 (2)	C(2)–C(1)–C(6)	126 (2)	C(1)–C(2)–C(3)	115 (2)
C(2)–C(3)–C(4)	121 (2)	C(3)–C(4)–C(5)	118 (2)	C(3)–C(4)–C(7)	127 (2)	C(5)–C(4)–C(7)	114 (2)
C(4)–C(5)–C(6)	119 (2)	C(1)–C(6)–C(5)	119 (2)	C(4)–C(7)–O(1)	124 (2)	C(4)–C(7)–N_1	117 (2)
O(1)–C(7)–N_1	119 (2)	C_8^{α}–C_8'O(2)	111 (2)	O_8–C_8'–O(2)	121 (2)	C_8'–O(2)–C(8)	124 (2)
O(2)–C(8)–C(9)	104 (2)	O(2)–C(8)–C(10)	110 (2)	O(2)–C(8)–C(11)	108 (2)	C(9)–C(8)–C(10)	111 (3)
C(9)–C(8)–C(11)	109 (3)	C(10)–C(8)–C(11)	114 (3)				

Table V

Torsion Angles (Deg) with ESD's for the Aib Residues in *p*-BrBz-$(Aib)_8$-O-*t*-Bu

angle	residue 1	2	3	4	5	6	7	8
C_i^{α}–C_i'–N_{i+1}–C_{i+1}^{α} (ω)	176 (2)	−177 (3)	180 (3)	−178 (2)	179 (2)	180 (3)	179 (2)	−179 (2)
C_{i-1}'–N_i–C_i^{α}–C_i' (ϕ)	56 (2)	49 (2)	47 (2)	53 (2)	52 (2)	58 (2)	62 (2)	−57 (2)
N_i–C_i^{α}–C_i'–N_{i+1} (ψ)	39 (2)	31 (2)	26 (2)	30 (2)	30 (2)	24 (2)	19 (2)	−46 (2)
O_{i-1}–C_{i-1}'–N_i–C_i^{α}	−7 (2)	4 (2)	12 (2)	0 (2)	0 (2)	1 (2)	−3 (2)	6 (2)
C_{i-1}'–N_i–C_i^{α}–$C_i^{\beta,L}$	−64 (2)	−74 (2)	−69 (2)	−72 (2)	−69 (2)	−74 (2)	−65 (2)	−172 (2)
C_{i-1}'–N_i–C_i^{α}–$C_i^{\beta,D}$	178 (2)	166 (2)	169 (33)	162 (2))	172 (2)	169 (2)	172 (2)	65 (2)
N_i–C_i^{α}–C_i'–O_i	−149 (2)	−158 (2)	−154 (2)	−148 (3)	−152 (2)	−155 (2)	−168 (2)	136 (3)
$C_i^{\beta,L}$–C_i^{α}–C_i'–N_{i+1}	158 (2)	156 (2)	140 (2)	159 (2)	153 (2)	154 (3)	147 (2)	68 (2)
$C_i^{\beta,D}$–C_i^{α}–C_i'–N_{i+1}	−81 (2)	−84 (2)	−97 (2)	−83 (2)	−90 (2)	−86 (2)	−94 (2)	−169 (2)
$C_i^{\beta,L}$–C_i^{α}–C_i'–O_i	−29 (2)	−33 (2)	−40 (2)	−19 (2)	−29 (2)	−25 (2)	−40 (2)	−109 (3)
$C_i^{\beta,D}$–C_i^{α}–C_i'–O_i	92 (2)	87 (2)	83 (3)	99 (3)	88 (3)	96 (2)	79 (2)	14 (3)

Torsion Angles (Deg) with ESD's for the N- and C-Terminal Blocking Groups of *p*-BrBz-$(Aib)_8$-O-*t*-Bu

O(1)–C(7)–C(4)–C(3)	−155 (3)	O(1)–C(7)–C(4–)C(5)	13 (2)	N_1–C(7)–C(4)–C(3) (θ_1)	26 (2)
N_1–C(7)–C(4–)C(5) (θ_2)	−167 (3)	C_1^{α}–N_1–C(7)–C(4) (ω_0)	173 (2)	C(8)–O(2)–C_8'–O_8	−2 (2)
C(9)–C(8)–O(2)–C_8'	175 (3)	C(10)–C(8)–O(2)–C_8'	56 (2)	C(11)–C(8)–O(2)–C_8'	−69 (2)

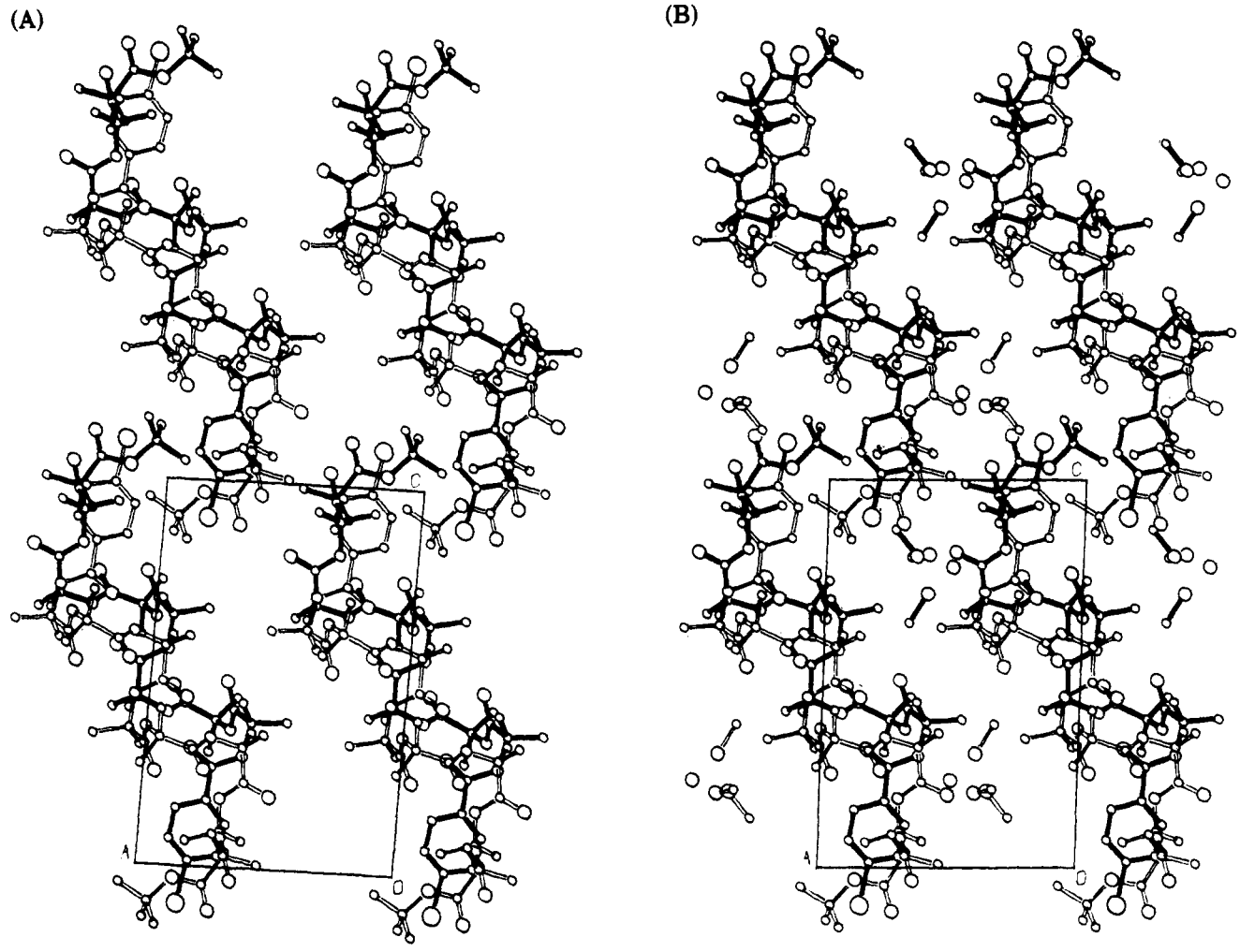

Figure 5. (A) Mode of packing of the *p*-BrBz-$(Aib)_8$-O-*t*-Bu molecules as projected down the *b* axis. (B) Mode of packing of the same molecules in the unit cell together with the solvent molecules (3 methanol and 1 water molecules).

turn. The separation of the methyl groups of one residue from the methyl groups on both adjacent turns of the helix is 4.6 Å. The sign of the ϕ,φ torsion angles of the last Aib residue of the octapeptide, Aib(8), is opposite to those of the preceding residues (Table V), a common feature of the structures of Aib homopeptides.[3,44,52,56,61]

The amide group of the N-terminal *p*-bromobenzoyl moiety is trans and slightly distorted from planarity (ω_0 = −172.5°); the torsion angles involving the amide group and the ortho carbon atoms of the aromatic ring, θ_1 and θ_2, have values of −25.8° and +166.7°, respectively (Table V).[37,48] The O-*t*-Bu ester group adopts a conformation with respect to the C_8^{α}–N_8 bond close to the anticlinal conformation, the O_8–C_8'–C_8^{α}–N_8 torsion angle being −136.4°.[16,51] Interestingly, the intermolecular H-bonding scheme does not involve any such bond between peptide molecules in the unit cell (Table VI and Figure 5). However, H bonds are observed between the N_1, N_2, O_6, O_7, and O_8 atoms of the peptide (not involved in the intramolecular H-bonding scheme) and the cocrystallized

Table VI
Intra- and Intermolecular H Bond Distances in the Molecules of *p*-BrBz-(Aib)$_8$-O-*t*-Bu

donor	acceptor	distance, Å
(A) Intramolecular H Bonds		
N_8	O_5	3.00
N_7	O_4	3.03
N_6	O_3	2.96
N_5	O_2	3.00
N_4	O_1	2.94
N_3	O(1)	3.04
(B) Intermolecular H Bonds		
N_1	O_{M1}[a]	3.06
N_2	O_w[b]	2.96
O_{M1}	O_7	2.79
O_{M2}	O_6	2.79
O_{M3}	O_{M2}	2.75
O_w	O_8	2.81
O_w	O_{M3}	2.75

[a] M1, M2, and M3 indicate the three cocrystallized methanol molecules. [b] w indicates the cocrystallized water molecule.

solvent molecules (3 methanol and 1 water molecules). All donor and acceptor groups participate in the H-bonding scheme.

Along the $(a + c)$ direction helical rods of molecules, piled up in a head-to-tail fashion, are held together by N–H···O and O–H···O H-bonds and van der Waals contacts among hydrophobic groups. Along the *b* direction, nearly orthogonally to the axis of the molecules, the packing of the rods gives rise to a channel, in which the water and methanol molecules are accommodated. In the channel the solvent molecules are crystallographically ordered, being involved in H bonds with the octapeptide molecules. This situation is at variance with that observed in the solid state for other channel-forming hydrophobic peptides.[44]

4. Discussion

By means of conformational energy computations[1,4,10,33,38,40,42,60,61] it was determined that α-methyl substitution in the Ala residue would produce a strong conformational effect in the resulting Aib residue, restricting its ϕ,φ angles to values near those characteristic of either the 3_{10}- or the α-helix. In the early 1960s, Blout and Fasman[5] and Elliott et al.,[20] independently, from simple analyses of molecular models were able to show that unfavorable steric interactions are more serious in the α-helix of poly(Aib)$_n$ than in the 3_{10}-helix. However, solid-state studies on *polydispersed* poly(Aib)$_n$ were unable to provide a clear-cut answer to the problem of the type of helix which is formed.[17-19,30,31] Our recent IR absorption and ^{1}H NMR analyses of the preferred conformation of terminally blocked, *monodispersed* (Aib)$_n$ homooligopeptides to the dodecamer are strongly in favor of the onset of *fully* developed 3_{10}-helices in $CDCl_3$, starting from the octamer.[58] These results agree well with those reported by Paterson et al.[39] on Ac-(Aib)$_n$-NHMe (n = 1–3; Ac, acetyl; NHMe, methylamido). A comparison between the $CDCl_3$ solution and crystal-state results of *p*-BrBz-(Aib)$_8$-O-*t*-Bu described in this work allows us to conclude that this terminally blocked octapeptide forms a 3_{10}-helical structure insensitive to environmental effects. This conclusion supports the hypothesis that the Aib residue has an asymmetric geometry at the C^α atom in solution, analogous to that found in the crystal state.[39] The regular 3_{10}-helix formed by *p*-BrBz-(Aib)$_8$-O-*t*-Bu is stabilized by six consecutive intramolecular H bonds of the helical C_{10}-type (III or III′).[53,55,62] We believe that our results, taken together, represent a decisive proof in favor of the 3_{10}-helix as a preferred conformation of poly(Aib)$_n$, and that main-chain length may *not* be an overriding factor in directing the helical folding in these homopeptides. In this work, which describes at atomic resolution a *regular* 3_{10}-helix larger than two complete turns, we characterize in detail for the first time this important peptide secondary structure.[13,34,47,49] The mean value of the ϕ,φ, and ω angles are ±54.0°, ±28.4°, and ±178.3°, respectively. The mean value of the N···O distance of the intramolecular H bonds of the helical C_{10}-type (III or III′) is 2.99 Å. The pitch of this helical structure is 5.85 Å. Interestingly, packing of the octapeptide molecules forms a channel, in which the solvent (methanol and water) molecules are accommodated.

References and Notes

(1) Balaram, P. In "Peptides: Structure and Function"; Hruby, V. J., Rich, D. H., Eds.; Pierce Chemical Co.: Rockford, IL, 1983; pp 477–486.
(2) Benedetti, E. in "Chemistry and Biochemistry of Amino Acids, Peptides, and Proteins"; Weinstein, B., Ed.; Marcel Dekker: New York, 1982; pp 105–184.
(3) Benedetti, E.; Bavoso, A.; Di Blasio, B.; Pavone, V.; Pedone, C.; Crisma, M.; Bonora, G. M.; Toniolo, C. *J. Am. Chem. Soc.* **1982**, *104*, 2437–2444.
(4) Benedetti, E.; Toniolo, C.; Hardy, P.; Barone, V.; Bavoso, A.; Di Blasio, B.; Grimaldi, P.; Lelj, F.; Pavone, V.; Pedone, C.; Bonora, G. M.; Lingham, I. *J. Am. Chem. Soc.* **1984**, *106*, 8146–8152.
(5) Blout, E. R.; Fasman, G. D., locally cited in ref 20.
(6) Bonora, G. M.; Mapelli, C.; Toniolo, C.; Wilkening, R. R.; Stevens, E. S. *Int. J. Biol. Macromol.* **1984**, *6*, 179–188.
(7) Bonora, G. M.; Toniolo, C.; Di Blasio, B.; Pavone, V.; Pedone, C.; Benedetti, E.; Lingham, I.; Hardy, P. *J. Am. Chem. Soc.* **1984**, *106*, 8152–8156.
(8) Bosch, R.; Jung, G.; Schmitt, H.; Winter, W. *Biopolymers* **1985**, *24*, 961–978.
(9) Bosch, R.; Jung, G.; Schmitt, H.; Winter, W. *Biopolymers* **1985**, *24*, 979–999.
(10) Burgess, A. W.; Leach, S. J. *Biopolymers* **1973**, *12*, 2599–2605.
(11) Chandrasekaran, R.; Mitra, A. K. In "Conformation in Biology"; Srinivasan, R., Sarma, R. H., Eds.; Adenine Press: Guilderland, NY, 1983; pp 91–98.
(12) Cromer, D. T.; Waber, J. T. In "International Tables for X-Ray Crystallography"; Kynoch Press: Birmingham, U.K., 1974; Vol. 4, Table 2.2B.
(13) Dickerson, R. E.; Geis, I. In "The Structure and Actions of Proteins"; Harper and Row: New York, 1969.
(14) Dijkstra, B. W.; Renetseder, R.; Kalk, K. H.; Hol, W. G. J.; Drenth, J. *J. Mol. Biol.* **1983**, *168*, 163–179.
(15) Donohue, J. *Proc. Natl. Acad. Sci. U.S.A.* **1953**, *39*, 470–478.
(16) Dunitz, J. D.; Strickler, P. In "Structural Chemistry and Molecular Biology"; Rich, A., Davidson, N., Eds.; W. H. Freeman: San Francisco, 1968; pp 595–602.
(17) Dwivedi, A.; Krimm, S.; Malcolm, B. R. *Biopolymers* **1984**, *23*, 2025–2065.
(18) Elliott, A. *Proc. R. Soc. London, Ser. A* **1954**, *226*, 408–421.
(19) Elliott, A.; Malcolm, B. R. *Trans. Faraday Soc.* **1956**, *52*, 528–536.
(20) Elliott, A.; Bradbury, E. M.; Downie, A. R.; Hanby, W. E. In "Polyamino Acids, Polypeptides and Proteins"; Stahmann, M. A., Ed., The University of Wisconsin Press: Madison, WI, 1962; pp 255–273.
(21) Flippen, J. L.; Karle, I. L. *Biopolymers* **1976**, *15*, 1081–1092.
(22) Fox, R. O., Jr.; Richards, F. M. *Nature (London)* **1982**, *300*, 325–330.
(23) Francis, A. K.; Iqbal, M.; Balaram, P.; Vijayan, M. *FEBS Lett.* **1983**, *155*, 230–232.
(24) Germain, G.; Main, P.; Woolfson, M. M. *Acta Crystallogr., Sect. A* **1971**, *27*, 368–376.
(25) IUPAC–IUB Commission on Biochemical Nomenclature *Biochemistry* **1970**, *9*, 3471–3479.
(26) Jung, G.; Brückner, H.; Schmitt, H. in "Structure and Activity of Natural Peptides"; Voelter, W., Weitzel, G., Eds.; de Gruyter: Berlin, 1981; pp 75–114.
(27) Kamphuis, I. G.; Kalk, K. H.; Swarte, M. B. A.; Drenth, J. *J. Mol. Biol.* **1984**, *179*, 233–256.
(28) Karle, I. L. In "The Peptides: Analysis, Structure, Biology"; Gross, E., Meienhofer, J., Eds.; Academic Press, New York, 1981; pp 1–54.
(29) Kopple, K. D.; Schamper, T. J. *J. Am. Chem. Soc.* **1972**, *94*, 3644–3646.
(30) Malcolm, B. R. *Biopolymers* **1977**, *16*, 2591–2592.

(31) Malcolm, B. R. *Biopolymers* **1983**, *22*, 319–322.
(32) Martin, D.; Hauthal, G. In "Dimethyl Sulphoxide"; van Nostrand-Reinhold: Wokingham, England, 1975.
(33) Marshall, G. R. In "Intra-Science Chemistry Report"; (Kharasch, N., Ed.; Gordon and Breach: New York, 1971; Vol. 5, pp 305–316.
(34) Matthews, B. W. In "The Proteins", 3rd ed.; Neurath, H., Hill, R. L., Boeder, C. L., Eds.; Academic Press: New York, 1977; Vol. III, pp 403–590.
(35) Mizushima, S.; Shimanouchi, T.; Tsuboi, M.; Souda, R. *J. Am. Chem. Soc.* **1952**, *74*, 270–271.
(36) Nagaraj, R.; Balaram, P. *Acc. Chem. Res.* **1981**, *14*, 356–362.
(37) Nakamura, H.; Morishima, H.; Takita, T.; Umezawa, H.; Iitaka, Y. *J. Antibiot.* **1973**, *26*, 255–256.
(38) Paterson, Y.; Rumsey, S. M.; Benedetti, E.; Némethy, G.; Scheraga, H. A. *J. Am. Chem. Soc.* **1981**, *103*, 2947–2955.
(39) Paterson, Y.; Stimson, E. R.; Evans, J. D.; Leach, S. J.; Scheraga, H. A. *Int. J. Pept. Protein Res.* **1982**, *20*, 468–480.
(40) Peters, D.; Peters, J. *J. Mol. Struct.* **1982**, *86*, 341–347.
(41) Pitner, T. P.; Urry, D. W. *J. Am. Chem. Soc.* **1972**, *94*, 1399–1400.
(42) Pletnev, V. Z.; Gromov, E. P.; Popov, E. M. *Khim. Prir. Soedin.* **1973**, *9*, 224–229.
(43) Pulla Rao, Ch.; Nagaraj, R.; Rao, C. N. R.; Balaram, P. *Biochemistry* **1980**, *19*, 425–431.
(44) Pulla Rao, Ch.; Shamala, N.; Nagaraj, R.; Rao, C. N. R.; Balaram, P. *Biochem. Biophys. Res. Commun.* **1981**, *103*, 898–904.
(45) Pysh, E. S.; Toniolo, C. *J. Am. Chem. Soc.* **1977**, *99*, 6211–6219.
(46) Ramakrishnan, C.; Prasad, N. *Int. J. Pept. Protein Res.* **1971**, *3*, 209–231.
(47) Richardson, J. S. *Adv. Protein Chem.* **1981**, *34*, 167–339.
(48) Robert, F.; Jeannin, Y.; Vincent, M.; Laubie, M. *Acta Crystallogr., Sect. C* **1984**, *40*, 1219–1220.
(49) Schellman, Ch. In "Protein Folding"; Jaenicke, R., Ed.; Elsevier: Amsterdam, 1980; pp 53–61.
(50) Schmitt, H.; Winter, W.; Bosch, R.; Jung, G. *Liebigs Ann. Chem.* **1982**, 1304–1321.
(51) Schweizer, R.; Dunitz, J. D. *Helv. Chim. Acta* **1982**, *65*, 1547–1554.
(52) Shamala, N.; Nagaraj, R.; Balaram, P. *J. Chem. Soc., Chem. Commun.* **1978**, 996–997.
(53) Smith, J. A.; Pease, L. G. *CRC Crit. Rev. Biochem.* **1980**, *8*, 315–398.
(54) Stevens, E. S.; Sugawara, W.; Bonora, G. M.; Toniolo, C. *J. Am. Chem. Soc.* **1980**, *102*, 7048–7050.
(55) Toniolo, C. *CRC Crit. Rev. Biochem.* **1980**, *9*, 1–44.
(56) Toniolo, C.; Bonora, G. M.; Bavoso, A.; Benedetti, E.; Di Blasio, B.; Pavone, V.; Pedone, C. *Biopolymers* **1983**, *22*, 205–215.
(57) Toniolo, C.; Bonora, G. M.; Bavoso, A.; Benedetti, E.; Di Blasio, B.; Pavone, V.; Pedone, C. *J. Biomol. Struct. Dyn.*, submitted.
(58) Toniolo, C.; Bonora, G. M.; Bavoso, A.; Benedetti, E.; Di Blasio, B.; Grimaldi, P.; Lelj, F.; Pavone, V.; Pedone, C. *Macromolecules*, **1985**, *18*, 895–902.
(59) Valle, G.; Toniolo, C., manuscript in preparation.
(60) Venkataram Prasad, B. V.; Sasisekharan, V. *Macromolecules* **1979**, *12*, 1107–1110.
(61) Venkataram Prasad, B. V.; Balaram, P. *CRC Crit. Rev. Biochem.* **1984**, *16*, 307–348.
(62) Venkatachalam, C. M. *Biopolymers* **1968**, *6*, 1425–1436.
(63) Venkatachalam, C. M.; Ramachandran, G. N. In "Conformation of Biopolymers"; Ramachandran, G. N., Ed.; Academic Press: New York, 1967; pp 83–105.
(64) Wilkening, R. R.; Stevens, E. S.; Bonora, G. M.; Toniolo, C. *J. Am. Chem. Soc.* **1983**, *105*, 2560–2561.
(65) Wlodawer, A.; Walter, J.; Huber, R.; Sjölin, L. *J. Mol. Biol.* **1984**, *180*, 301–329.

Notes

X-ray Powder Diffractograms of Some Oligo- and Poly(1,1′-ferrocenylenes)†

EBERHARD W. NEUSE*

Department of Chemistry, University of the Witwatersrand, Johannesburg 2000, Republic of South Africa

STEWART HART

National Institute for Materials Science, Pretoria 0001, Republic of South Africa. *Received April 18, 1985*

Yamamoto and Collaborators recently described the preparation[1] and properties[2] of a linear, yet benzene-insoluble, poly(1,1′-ferrocenylene) (1) said to possess a molecular mass of 4600 (i.e., $\bar{n} \simeq 25$) and show crystallinity as determined by X-ray powder diffractometry. These

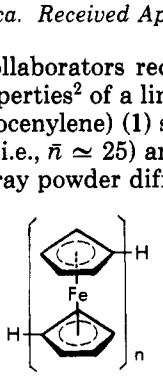

findings appeared doubtful in light of the excellent solubility in aromatic solvents observed in extended previous work[3-5] for pure, linear 1 in the molecular mass range 1500–6000 and higher. Because of the overriding importance of solubility for the analytical characterization and use of polymers of this type, we decided to clarify this inconsistency of observations by determining the crystallinity of authentic, soluble poly(1,1′-ferrocenylene) fractions with molecular masses extending up to 5000 for comparison with the diffractometric findings of Yamamoto et al.[2]

Authentic 1 was synthesized by the organolithium–organohalide coupling method as previously described.[5] The crude polymer was fractionated by the earlier established[5] procedure to give, in the order of decreasing degree of polymerization, the polymeric fractions I and II and the oligomer fractions III and IV. Fraction I was further fractionated, by fractionating precipitation,[5] into six subfractions, four of which, labeled Ia, Ib, Ic, and Id, were included in the subsequent evaluation. Molecular mass data and benzene-solubility properties were determined for fractions Ia–d as well as for III and IV. The results are given in Table I. X-ray powder diffractograms (Cu Kα) were recorded within the range 2θ = 10–30° for fractions Ia–d and III, as well as for a tetracyanoquinodimethanide ($TCNQ^-$) polysalt of III prepared as described in Yamamoto's paper.[2] Prominent *d* spacings derived from the diagrams for Id (very weak signals) and III (moderately strong signals) are included in Table I, and the well-developed diffractogram of the TCNQ salt of fraction III is summarized in Table III. No signals were detectable for fractions Ia–c.

Next, a poly(ferrocenylene) was synthesized from 1,1′-dibromoferrocene and magnesium in THF–dibromoethane as described in the first paper[1] of Yamamoto's group. The crude product was fractionated by the same procedure as used for the isolation of the fractions in Table I. Low degrees of polymerization and correspondingly poor yields in soluble higher molecular material necessitated per-

† Metallocene Polymers, 42.

0024-9297/86/2219-0479$01.50/0